NUCLEATION AND GRAIN GROWTH OF REDUCED METALLIC IRON AT 900 - 1100°C

A.A. El-Geassy, M.I. Nasr and I.F. Hewady

Central Metallurgical Research and Development Institute, El-Tabbin, Egypt

Abstract

Iron oxide was isothermally reduced to metallic iron at 900-1100°C in hydrogen, carbon monoxide and their mixtures. Thermogravimetric technique was used for accurate determination of oxygen weight loss during reduction as a function of time. The reduced samples were examined with light and scanning electron microscopes. X-ray and carbon analyses were also used. In H_2, metallic iron was nucleated allover the iron oxide surface even at the early stages of reduction, while, on the other hand, in CO the iron was nucleated partially on the oxide surface, even at the latter stages of reduction. Unlike in H_2, the reduction with CO shows the presence of an incubation period at low pressure which delays the reduction and formation of iron nuclei. The grain growth of iron nuclei due to further reduction was higher in CO than in H_2. The influence of total pressure on the nucleation, grain growth and incubation period was investigated. The presence of silica enhanced nucleation in CO than H_2.

Introduction

The gaseous reduction of iron oxides is of practical importance in view of the current interest in direct reduction processes. Many investigators have used reagent grade materials either to eliminate the influence of the impurities present in natural ores or to determine the effect of these impurities by making appropriate addition. During the reduction of Fe_2O_3 by either H_2, CO, H_2- CO mixtures or solid carbon to metallic iron an intermediate oxides of iron are present such as magnetite and wustite phases. Some authors have observed an initial period during which the rate of reduction increases to a maximum(1-3). This period referred to as "induction period", is generally attributed to non-uniform nucleation. In some cases, a delay in the reduction period referred to as "incubation period" during which no measurable amounts of reduction has been observed (4). This period could be caused by an activation energy barrier to nucleation. As a result of structural changes during reduction, different reduction models have been proposed and discussed (5, 6).

Method of Physical Characterization of Solids

Partially and completely reduced micropellets of W.1 and W.2 were examined with optical microscope (LM) and scanning electron microscope (SEM), type Cambridge Sterioscan 600, UK. X-ray diffraction technique was also applied.

The surface structure of W.1 and W.2, as was examined by SEM, is shown in Fig. 2(a) and (b) respectively. It can be observed that, unlike W.2, W.1 exhibited a faceted structure while W.2 showed more porous structure due to the presence of silica which counteracts sintering and recrystallization of wustite grains. Moreover X-ray analysis of W.1 and W.2 indicated the presence of fayalite ($2\ FeO.SiO_2$) only in W.2 while W.1 is composed of wustite. This fayalite resulted from the reaction between silica (SiO_2) and wustite;

$$2\ FeO + SiO_2 \longrightarrow 2\ FeO.\ SiO_2$$

The specific surface area of W.1 and W.2, measured by the aid of BET technique, is 0.0580 and 1.1218 m^2/gm respectively. The higher value of W.2 than W.1 can be attributed to its porous structure (Fig. 2b) and the presence of fayalite.

Results and Discussion

Kinetics of Reduction

200 ug of either W.1 and W.2 were isothermally reduced at 900, 950, 1000, 1050 and 1100°C in H_2, CO and H_2- CO mixtures. The reduction curves were previously given(9). The calculated rate of reduction (dR/dt), calculated from the reduction curves, was plotted against the corresponding reducing gas composition as shown in Figs. 3 and 4 for W.1 and W.2 respectively. These showed that the rate of reduction (dR/dt) decreased with increasing the CO content in the gas mixture. Unlike W.2, W.1 shows an abrupt decrease in the rate of reduction in 97.5% CO + 2.5% H_2 gas mixture. The effect of addition of H_2 to CO on the rate of reduction of W.1 at various pressures (0.1 up to 1.0 atm.) with different reducing gas mixtures is shown in Fig. 5. In H_2 and H_2- containing gas mixtures a linear relationship between the rate of reduction (R) and the H_2 content in the gas mixture ($\%X_{H_2}$), may have the form;

$$\ln (R)_{Mixture} = -A\ X_{H_2} + \ln (R)H_2 \qquad (1)$$

where; A is a constant and $(R)_{H_2}$ is the rate in pure hydrogen.

This relationship was valied at all temperatures and pressures for W.2, while on the other hand, in case of W.1 this relationship was valied up to 2.5% H_2- containing gas mixtures and below which an abrupt decrease in the rate was obtained as shown in Fig. 3.

On the other hand, the photomicrographs of W.2 micropellets at higher extents of reduction (75%), Fig. 10, showed a shrinking **core** model type of reaction. H_2 and H_2- CO mixtures, no sharp interface between iron and wustite is obtained. In CO reduction a very sharp interface is found and a complete coverage of wustite surface with a uniform layer of iron was formed and consequently the growths of iron can take place by solid-state diffusion mechanism.

The nature of reducing gas composition has a great influence on the shape and distribution of the formed iron nuclei on the wustite surface. For W.2 the reduction in H_2 and H_2- rich gas mixtures ($\geq$75% H_2), several iron nuclei exhibited hexagonal shape and triangular pores can be observed (Fig. 7a, b). While in CO reduction iron whiskers were formed at the early stages of reduction (Fig. 7c). The formation of these iron whiskers can be formed through a combined effect of nucleation and growth of iron on some active sites where fayalite (2 FeO. SiO_2) is present. This fayalite was formed through reaction between wustite and silica. With progress of reduction the iron covered the entire surface of wustite grains independent on the reducing gas composition. These iron whiskers disappeared due to sintering effect as shown in Fig. 11.

X-ray analysis of the reduced samples of W.1 and W.2 showed the presence of iron carbides and α-Fe. The formation of iron carbides was previously described (reactions 2 and 3).

Effect of Total Pressure

The effect of total pressure of reducing gas on the behaviour of nucleation and grain growth of iron was studied at 1000°C using micropellets of W.1. The relationship between the rate of reduction (dR/dt), at the initial stages (5% red.) and the corresponding gas composition at different pressures (0.1 up to 1.0 atm.) is shown in Fig. 5. It shows that in H_2 and H_2- containing gas mixtures, a linear relationship was obtained. In CO, on the other hand an abrupt decrease in the rate was observed. This was attributed to the poisoning effect of CO molecules on the wustite surface(9), which hinders reduction thus giving lower rate of reduction. This effect decreases the rate and number of iron nuclei on the wustite surface. The SEM photomicrographs of W.1 micropellets partially reduced (25%) in H_2 and in CO at reduced pressure (0.25 atm.) are shown in Fig. 12(a) and (b) respectively. It shows that, while the entire surface of grains is nucleated with iron in H_2, the surface is partially nucleated with iron in carbon monoxide showing larger growth than that in hydrogen.

The variation between the rate of reduction with H_2, CO and H_2- CO mixtures and the total pressure on log-log scale, as shown in Fig. 13, is obtained from the relationship:

$$(R) = K A P^n \qquad (2)$$

Incubation Period and Mechanism of Nucleation and Growth of Iron

A feature of the reduction of wustite micropellets (W.1) with carbon monoxide at 0.1 up to 1.0 atmosphere, is the presence of an incubation period which decreases with increase in the total pressure of CO, as shown in Fig. 15. The relationship between the incubation period (t_{inc} in seconds) and the total pressure of carbon monoxide (P_{CO} in atm.) can be represented by;

$$t_{inc} = Ae^{-BP_{CO}} \quad (3)$$

where; A and B are constants. Fig. 16 showsthe relationship between (t_{inc}) and P_{CO} in log-log plots. A straight line wasobtained from which;

$$t_{inc} = 10\, e^{-1.26\, P_{CO}} \quad (4)$$

On the other hand, this incubation period was not observed in case of reduction with pure hydrogen or H_2- containing gas mixtures. This indicates that the mechanism of nucleation and reduction is reducing gas composition dependent.

The presence of an incubation period which delays nucleation and consequently the reduction at the initial stages is caused by the following factors(8), which influence nucleation of iron on the wustite surface:

a. The minimum energy required to form a nucleus with a critical size.
b. The concentration of favourable sites.
c. The rate of surface reaction.
d. The rate of atomic rearrangements in the lattice.

The free energy change associated with the formation of a spherical nucleus of a solid phase (I) with radius r, in a solid phase (II), is give by(12);

$$G(r) = \frac{4}{3}\pi r^3 (\Delta G_V - \Delta G_E) + 4\pi r^2 \gamma \quad (5)$$

where ΔG_V and ΔG_E are the free energy and the strain energy per unit volume and γ is the net surface energy per unit area of the new phase. Of the terms on the right hand side of equation (5) only ΔG_V is negative. It can be shown that for a nucleus to grow it must be greater than a critical size given by:

$$r_C = \frac{-2\gamma}{\Delta G_V + \Delta G_E} \quad (6)$$

A minimum energy, ΔG_C, required for the growth of nucleus is obtained from equations (5) and (6):

4. Khalafalla, S.E., Reimers, G.W. and Baird, M.J. Met. Trans., 5, 1013, (1974).
5. Turkdogan, E.T. and Vinters, J.V. Met. Trans., 5, 11, (1974).
6. Szekely, J. and El-Tawil, Y. Met. Trans., 7B, 490 (1976).
7. Edstrom, J.O. Jerkont. Ann. 141, 809, (1957).
8. Sadrehashemi, F. "The reduction of hematite to magnetite in hydrogen-water vapour mixtures". Ph.D. Thesis, London Univ. (1977).
9. El-Geassy, A.A. and Rajakumar, V. JISI., 25, 449, (1985).
10. El-Geassy, A.A. JISI., 25, 1036 (1985).
11. El-Geassy, A.A. and Rajakumar, V. JISI., 25. 1202 (1985).
12. Shewmon, P.G. "Transformation in metals"., McGraw-Hill, New York, (1969).
13. Kohl, HK. and Engell, H.J. Arch. Eisenhuttenw., 34, 411, (1966).

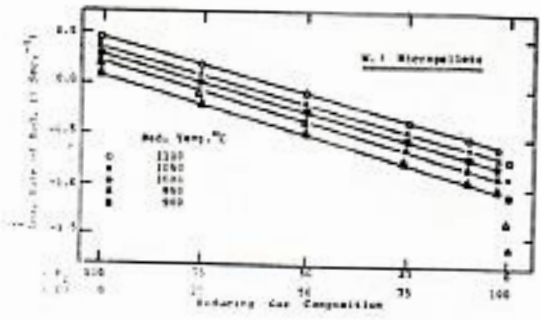

Fig.(3) Relationship between the log. of the Initial Rate of Reduction and the Reducing Gas Composition at 900-1100°C.

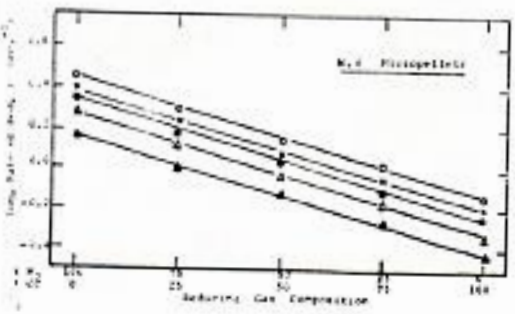

Fig.(4) Relationship between the log. of the Initial Rate of Reduction and the Reducing Gas Composition at 900-1100°C.

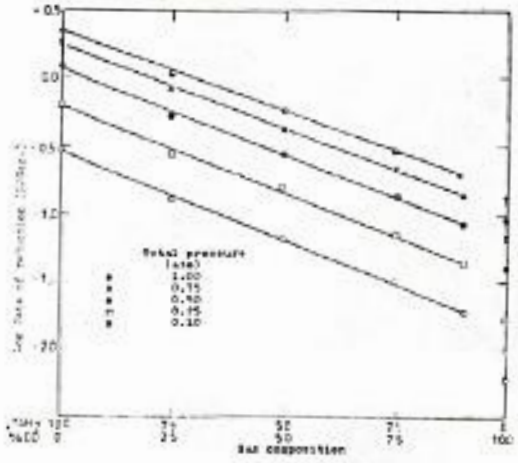

Fig.(5) Relationship between the initial rate of reduction and the reducing gas composition at various total pressure at 1000°C

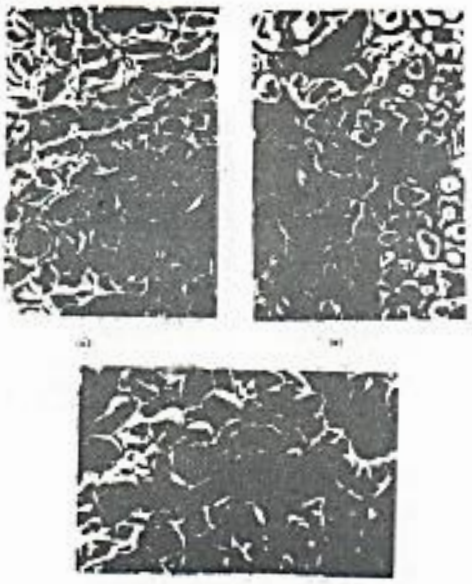

Fig.(6) Photomicrographs (SEM) of W.1 micropellets, 25% reduction at 1000°C with: (a) H_2 (b) 50% H_2 + 50% CO Mix. (c) CO

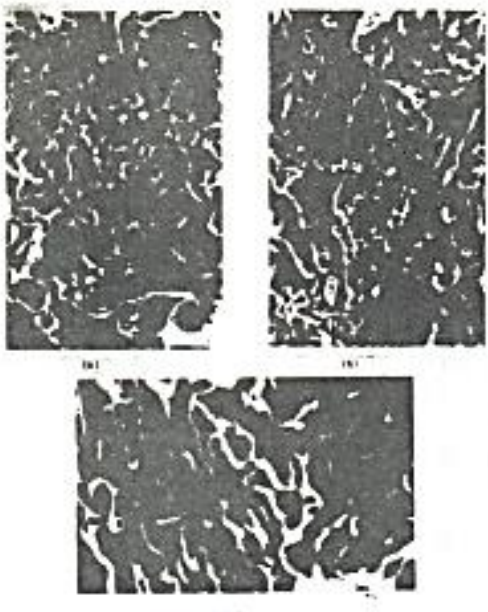

Fig. 11 Photomicrographs (SEM) of W.2 micropellets, 75% reduction at 1000°C with: (a) H_2 (b) 50% H_2 + 50% CO Mix. (c) CO

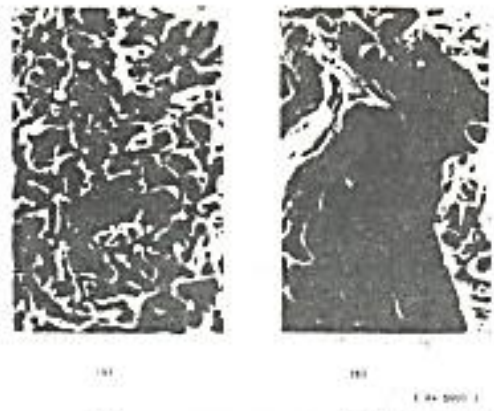

Fig.(12) Photomicrographs (SEM) of W.1 micropellets, 25% reduction at 1000°C in reduced pressure (0.25 atm.) with: (a) H_2 (b) CO

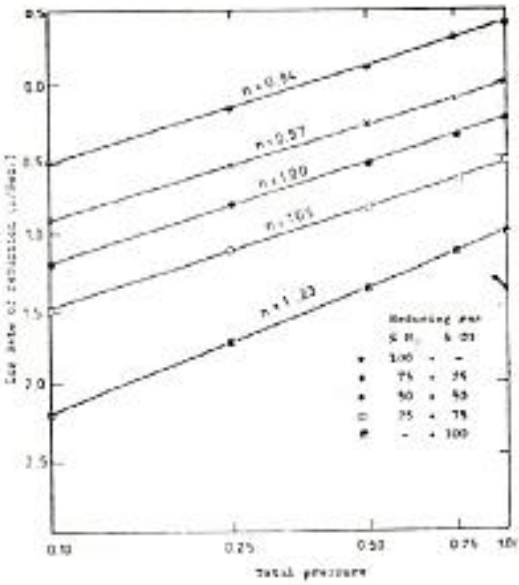

Fig.(13) Dependance of the log initial rate of reduction at 1000°C on the total gas pressure for wustite. 1 micropellets.

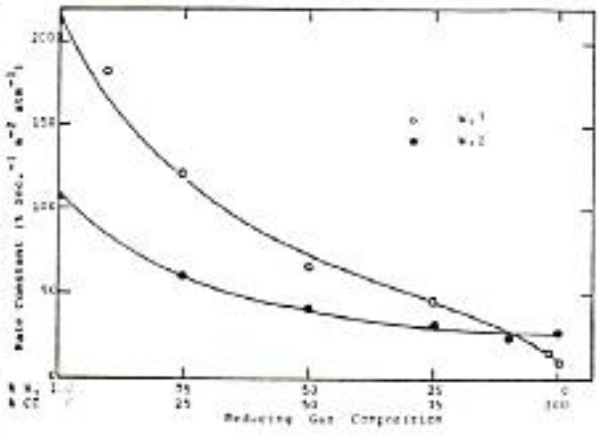

Fig.(14) Relationship between rate constant of W.1 and W.2 and the corresponding gas composition at 1000°C.